SARS-CoV-2 nucleocapsid protein promotes self-deacetylation by inducing HDAC6 to facilitate viral replication

Arpita Mukherjee[1], Mahadeb Lo[1], Pritam Chandra[1], Ratul Datta Chaudhuri[1], Papiya De[1], Shanta Dutta[1] and Mamta Chawla-Sarkar[1*]

Abstract

Background The global outbreak of COVID-19 caused by the SARS-CoV-2 has led to millions of deaths. This unanticipated emergency has prompted virologists across the globe to delve deeper into the intricate dynamicity of the host-virus interface with an aim to identify antiviral targets and elucidate host and viral determinants of severe disease.

Aim The present study was undertaken to analyse the role of histone deacetylase 6 (HDAC6) in regulating SARS-CoV-2 infection.

Results Gradual increase in HDAC6 expression was observed in different SARS-CoV-2-permissive cell lines following SARS-CoV-2 infection. The SARS-CoV-2 nucleocapsid protein (N protein) was identified as the primary viral factor responsible for upregulating HDAC6 expression. Downregulation of HDAC6 using shRNA or a specific inhibitor tubacin resulted in reduced viral replication suggesting proviral role of its deacetylase activity. Further investigations uncovered the interaction of HDAC6 with stress granule protein G3BP1 and N protein during infection. HDAC6-mediated deacetylation of SARS-CoV-2 N protein was found to be crucial for its association with G3BP1.

Conclusion This study provides valuable insights into the molecular mechanisms underlying the disruption of cytoplasmic stress granules during SARS-CoV-2 infection and highlights the significance of HDAC6 in the process.

Keywords Deacetylation, Stress granules (SGs), SARS-CoV-2, HDAC6, G3BP1

Introduction

The emergence of COVID-19 pandemic caused by beta corona-virus SARS-CoV-2 resulted in 7,049,617 deaths till May, 2024 and continues to infect through evolution of new variants [53]. The clinical course of COVID-19 exhibits a broad spectrum of severity and progression patterns. While in a significant number of people, SARS-CoV-2 infection led to mild upper respiratory disease or even asymptomatic sub-clinical infection, others developed symptoms and complications of severe pneumonia [12].

The SARS-CoV-2 genome is composed of a single stranded 30 kb positive sense RNA which encodes for fourteen ORFs. The 5′ *orf1a*/*orf1ab* encodes polyproteins, which are auto-proteolytically processed into sixteen non-structural proteins (NSP1-16) which form the replicase/transcriptase complex (RTC) [6, 13]. The RTC consists several enzymes, including the papain-like protease (NSP3), the main protease (NSP5), the primary viral RNA-dependent RNA polymerase (NSP12), the NSP7-NSP8 primase complex, a helicase/triphosphatase (NSP13), an exoribonuclease (NSP14), an endonuclease (NSP15), and N7- and 2′O-methyltransferases (NSP10/

*Correspondence:
Mamta Chawla-Sarkar
chawlam70@gmail.com; chawlasarkar.m@icmr.gov.in
[1] Division of Virology, ICMR-National Institute of Cholera and Enteric Diseases, P-33, C.I.T. Road, Scheme-XM, Beliaghata, Kolkata, West Bengal 700010, India

Mukherjee *et al. Virology Journal*   (2024) 21:186

Page 2 of 16

NSP16). As many as thirteen ORFs are expressed from nine putative sub-genomic RNAs at the viral genome's 3' end. These include four structural proteins: Spike (S), Envelope (E), Membrane (M) and Nucleocapsid (N), and nine putative accessory factors [2, 57]. Once inside a cell, viruses interact with host proteins and hijacks complex cellular pathways to evade antiviral host defences and to facilitate viral propagation. For example, SARS-CoV-2 protein ORF9b antagonizes interferon response via preventing virus-induced K63 polyubiquitination of NFκB essential modulator (NEMO) [54]. On the other hand, SARS-CoV-2 protease NSP5 was found to evade RIG-I and MAVS signalling by cleaving ten N-terminal amino acids from RIG-I which renders it incapable of activating MAVS [31]. The SARS-CoV-2 NSP8 is also reported to localize to mitochondria to initiate mitophagy [65].

Histone deacetylases (HDACs) were initially recognized as enzymes that catalyse the removal of acetyl groups from the lysine residues present within histone proteins. Hence their role is extensively studied in the transcriptional regulation of genes. HDAC6, or Histone deacetylase 6, is a class II histone deacetylase enzyme and is unique among the HDACs because it is primarily localized within the cytoplasm and deacetylates non-histone proteins, such as tubulin, HSP90, Cortactin, RIG-I and β-Catenin [18, 24, 56, 58–60]. Interaction of HSP90 with HDAC6 have diverse outcomes ranging from apoptosis, autophagy, protein stability, cell migration, etc. [30]. In addition, HDAC6 has also been shown to be a component of cytoplasmic stress granules (SGs) and interacts with SG protein G3BP1. SGs are translationally stalled cytoplasmic mRNA–protein aggregates which are formed during various crises like oxidative stress, starvation, heat shock, infection with intracellular pathogens, etc. Once the stress is resolved mRNAs trapped within the SGs can again enter polysomes and resume translation. Viruses, especially cytoplasmic RNA viruses consider these SGs as potential threat and have devised multiple strategies to protect viral RNAs from being targeted by these cytoplasmic RNA granules [22, 37, 47, 50, 51].

HDAC6 inhibitors are currently undergoing clinical trials as potential therapeutics against several types of cancers, neurodegenerative disorders, and other chronic inflammatory diseases [44]. HDAC6 has lately been under investigations for its potential involvement in the regulation of various viral infections, including herpes simplex, ZIKA, Ebola, and the Sendai virus. Inhibition of HDAC6 activity has been shown to reduce viral replication in cells infected with ZIKA and HCV, suggesting that HDAC6 may be a potential target for antiviral drug designing [25, 45, 52]. Conversely, [64], reported a novel signalling pathway involving PKCα, HDAC6 and

β-catenin which was essential for IFN gene induction following Sendai virus infection. PKCα activation promotes HDAC6-mediated deacetylation of β-catenin, enhancing its nuclear translocation where it acts as co-activator for IRF3-mediated transcription. Moreover, during HIV infection, HDAC6 targets key viral proteins Pr55Gag and Vif for autophagic degradation, while protecting the stability and expression of the HIV-1 restriction factor APOBEC3G [33, 49]. According to a recent study, non-structural protein 5 (nsp5) of swine enteric coronaviruses employs a clever strategy to counteract the antiviral effect of HDAC6 by inducing the cleavage of HDAC6, thereby diminishing its antiviral role [28]. But, the role of HDAC6 in Influenza A virus (IAV) infection remains controversial. One study found that HDAC6 promotes IAV uncoating by facilitating aggresome formation [4]. In contrast, HDAC6 is claimed to suppress IAV replication by preventing acetylation of α -tubulin and viral RNA polymerase PA subunit [8].

The interaction between HDAC6 and viruses represent an active research area, and there is still much to learn about the precise mechanisms by which HDAC6 influences viral infections. In the present study we aimed to understand the role of HDAC6 in regulating SARS-CoV-2 infection.

Materials and methods
Cell lines, culture condition and viruses
A549 (human lung adenocarcinoma cells), VERO E6 (African green monkey kidney epithelial cells; ATCC®CCL-81™), and Calu-3 (human lung adenocarcinoma epithelial cells; ATCC® HTB-55™) cells were maintained in minimum essential medium (MEM, Gibco, USA) supplemented with 10% US-certified heat-inactivated FBS (Gibco, USA) and 1% antibiotic/antimycotic solution (Invitrogen, Carlsbad, CA, USA). Cells were maintained in a humidified incubator at 37 °C and with 5% CO_2. SARS-CoV-2 (GISAID accession id: EPI_ISL_430464 PANGO lineage: B.1.1 (Pango v.4.3 PANGO-v1.20) was isolated as a part of establishment of ICMR-COVID-19 biorepositories (Approval No. A-1/2020-IEC) [27]. Viral titre was determined using plaque assay [10]. VERO, and Calu-3 cells were infected with SARS-CoV-2 virus at a multiplicity of infection 1 and harvested at indicated time points post infection. A549 Cells were infected at a m.o.i. of 2 unless otherwise mentioned. In experiments that involved expression of HDAC6 catalytic mutant pcDNA-HDAC6.DC-FLAG, cells were infected at a m.o.i. of 0.5. All the experiments associated with virus infection were performed at Biosafety level 3 (BSL-3) laboratory and the study was approved by institutional Biosafety committee.

Mukherjee *et al. Virology Journal*   (2024) 21:186

Page 3 of 16

Estimation of infectious virus particle by plaque assay

Plaque assay was performed to estimate infectious virus particles. Confluent monolayers of VERO E6 cells grown in six-well plates were infected with serial dilutions (10^2–10^8) of viral supernatants and plaque assay was performed as previously described [48]. Viral plaque forming unit (PFU) was calculated as PFU/mL (Original stock) = {(1/dilution factor) × (number of plaques) × (1/[ml of inoculum/plate])} [3].

Quantitative real-time PCR

Total RNA was isolated from A549 cells using TRIzol (Invitrogen, Grand Island, USA) according to the manufacturer's instructions. Complementary DNA (cDNA) was synthesised from 1 μg of RNA using the Superscript II reverse transcriptase (Invitrogen) with random hexamer primers by incubating at 42 °C for 1 h. Real-time PCR was performed in triplicate using SYBR Green (Applied Biosystems, Foster City, CA, USA) in Step One Plus (Applied Biosystems). The temperature profile was set to 50 °C for 2 min, 95 °C for 10 min, followed by 40 cycles of 95 °C for 15 s, 60 °C for 30 s, and 72 °C for 10 s. The specific sets of primers used in this study are listed in Table 1. The viral gene expression was normalised with the expression of *gapdh* transcript using the formula $2^{-\Delta\Delta CT}$ ($\Delta\Delta CT = \Delta C_T$ Sample $- \Delta C_T$ Control), where C_T is the threshold cycle and the relative fold change in the viral transcript compared to *gapdh* transcript.

Western blot analysis

Protein lysates were prepared from harvested cells, washed once in phosphate-buffered saline (PBS), and lysed in Totex buffer (20 mM HEPES at pH 7.9, 0.35 M NaCl, 20% glycerol, 1% NP-40, 1 mM $MgCl_2$, 0.5 mM EDTA, 0.1 mM EGTA, 50 mM NaF and 0.3 mM Na_3VO_4) containing a mixture of protease and phosphatase inhibitors (Sigma-Aldrich, St. Louis, Missouri, USA). Protein concentration from whole cell lysate was measured using Bradford reagent and equal amount of protein lysate from each sample was mixed with sample buffer (final concentration: 50 mM Tris, pH 6.8, 1% SDS, 10% glycerol, 1% -mercaptoethanol and 0.01% bromphenol blue) and boiled for 5 min. Boiled cell lysates were subjected to SDS-PAGE and transferred to polyvinylidene difluoride (PVDF) membranes (Millipore). Membranes were then probed with the indicated primary antibodies. Primary antibodies were detected using horseradish peroxidase-conjugated secondary antibodies (Pierce, Rockford, IL, USA) and chemiluminescent substrate (Millipore, Billerica, MA, USA). Blots were re-probed with anti-GAPDH and anti β-actin antibodies to confirm equal protein loading. Blots were quantified using ImageJ software.

Cycloheximide chase assay

A549 cells either transfected with empty vector pcDNA3.1 or pcDNA3.1-N protein were treated with 10 μM cycloheximide to prevent cellular protein translation at 18 h post-transfection. Cycloheximide-treated plates were harvested after 6, 12, and 18 h post-cycloheximide treatment. In both the groups, mock-treated plates were harvested at the time of addition of cycloheximide in treated plates and designated as 0 h post-treatment.

Cloning of host and viral genes

Full length SARS-CoV-2 N gene was cloned into pcDNA3.1 /His B vector. Human pcDNA- HDAC6-FLAG and pcDNA-HDAC6.DC-FLAG [21] plasmids were purchased from Addgene (# 30482 and #30483). The plasmids pTwist-EF1alpha-SARS-CoV-2-S and pLVX-EF1alpha-nsp13 were generously provided by the Krogan lab [16].

Knockdown of HDAC6

pLKO.1-Puro (#8453, Addgene) lentiviral plasmid containing short hairpin sequences targeting HDAC6 was generated. pLKO.1-TRC cloning vector [35] was a gift from David Root (Addgene plasmid # 10878). For designing oligos, a siRNA selection programme hosted by Whitehead Institute for Biomedical Research hosts was accessed. HDAC6 knockdown efficiency was analysed via western blotting from cells expressing HDAC6 shRNA using HDAC6-specific antibody.

Immunofluorescence analysis

A549 cells were grown on glass coverslips with 40%-50% confluency and were transfected with pcDNA3.1 N protein followed by treatment with tubacin as mentioned in results section. Cells were subsequently fixed with 4%

Table 1 List of primers used in this study for the determination of cellular and viral transcript level by quantitative Real-time polymerase chain reaction

Gene names	Primer sequence	
gapdh	Forward primer	5′-GTCAACGGATTTGGTCGTATTG-3′
	Reverse primer	5′-TGGAAGATGGTGATGGGATTT-3′
hdac6	Forward primer	5′-ATGTTGGTTCACAGCCTAGAATA-3′
	Reverse primer	5′-CACAGGAGTATGAGTTCGGATG-3′
SARS-CoV-2 orf1a	Forward primer	5′-TTCTTGGTACAGGCTGGTAATG-3′
	Reverse primer	5′-GGTGTCTTAGGATTGGCTGTATC-3′

paraformaldehyde (dissolved in PBS) for 20 min. After 3–4 times wash with PBS, cells were permeabilised by using PBS containing 0.1% Triton X-100 (v/v) for 30 min. After permeabilisation, cells were blocked in blocking buffer (PBS supplemented with 2% bovine serum albumin [w/v]) for 1 h followed by overnight incubation with primary antibodies specific for N protein and G3BP1 at 4 °C. After 4–5 washes with PBS supplemented with 0.05% Triton X-100, cells were incubated with Rhodamine-labelled and/or DyLight488-labelled (Jackson Laboratories, Inc., West Grove, PA, USA) secondary antibodies in blocking buffer at room temperature for 1 h. After four washes with PBS containing 0.05% Triton X-100, cells were mounted with 4′, 6′ -diamidino-2-phenylindole (DAPI; [Vector Laboratories, Burlingame, CA, USA]) to visualize nucleus. Imaging was performed by using a Zeiss Axioplan microscope (63X oil immersion). To prevent cross-talk between fluorophores, the excitation and emission detection of each fluorophore was performed sequentially. Zen blue software was used to analyse the acquired images.

Plasmid transfection

Plasmids (pcDNA3.1-N protein, pcDNA-HDAC6-FLAG and pcDNA-HDAC6.DC-FLAG) were transfected in A549 cells using Lipofectamine 3000 (Invitrogen, USA). Control cells were transfected with empty vectors (designated as mock-transfected). In all experiments pcDNA3.1 empty vector was transfected as control.

Co-immunoprecipitation

Infected or transfected cells were washed with cold PBS and lysates were prepared. Protein concentration was measured by using Bradford reagent (Sigma-Aldrich, USA) and then equal quantities of protein lysates were clarified by incubation with protein A- Sepharose beads (GE Healthcare, Uppsala, Sweden) in 4 °C rotor for 2 h. After clarification, the protein A-Sepharose beads were removed by brief centrifugation and the supernatant was incubated with specific antibodies overnight at 4 °C, followed by incubation with protein A- Sepharose beads for 4 h. The beads were washed five times with 1X lysis buffer and the bound proteins were resolved in 10% SDS-PAGE. Subsequently, presence of specific protein in the immunoprecipitate was detected by Western blot analysis.

Reagents and antibodies

Tubacin (cat no. SML0065) and Cycloheximide (239763-M) were purchased from Sigma. $NaAsO_2$ (cat no. 35000-1L-R) was purchased from Thermo Fisher Scientific. Antibodies used in the study are listed in Table 2.

Statistical analysis

The data were expressed using the mean and standard deviation (SD) of at least three independent experiments (n = 3). To evaluate statistical significance, the unpaired Student's *t*-test was utilised. In all experiments, $p \leq 0.05$ was considered statistically significant.

Results

SARS-CoV-2 infection leads to the upregulation of Histone deacetylase 6 expression

To understand the involvement of HDAC6 in regulation of SARS-CoV-2 infection, we analysed the expression of HDAC6 during SARS-CoV-2 infection at different time points (18–40 h post infection) in VERO cells. Mock infected cells were harvested at each time points and run on the same gel. Western blot analysis showed time point-dependent progressive increase in HDAC6 protein level up to 32 h post infection (hpi) compared to respective mock infected controls (Fig. 1A). Next, we assessed the expression of HDAC6 in two other cell lines i.e., Calu-3 and A549. Consistently, SARS-CoV-2 infection of Calu3 cells showed increased expression of HDAC6 protein level up to 32 hpi followed by decrease at 40 hpi (Fig. 1B). However, A549 cells showed continuous increase in HDAC6 protein level up to 40 hpi which might be attributed to the moderate infectivity of SARS-CoV-2 in A549 cells [5], hence delayed progression of infection (Fig. 1C). Further experiments were done in A549 as these cells are easy to transfect and have been used previously in many studies [1, 5, 7, 40, 41]. To determine whether expression of HDAC6 is regulated during transcription, we infected A549 cells with SARS-CoV-2 followed by quantification using quantitative real-time PCR. Relative RNA level of *hdac6* compared to *gapdh* showed only a mild and inconsistent elevation of HDAC6 transcripts during the course of SARS-CoV-2 infection (Supplementary Fig. 1). The result is suggestive of post-transcriptional regulation of HDAC6 expression during SARS-CoV-2 infection.

Histone deacetylase 6 positively regulates SARS-CoV-2 propagation in vitro

In order to assess the functional significance of induction of HDAC6 expression in regulation of SARS-CoV-2 infection, A549 cells either transfected with shHDAC6 expressing plasmid or pcDNA-HDAC6-FLAG or mock transfected followed by SARS-CoV-2 infection (24 hpi) were subjected to quantitative real-time PCR using SARS-CoV-2 *orf1*, *hdac6* and *gapdh* specific primers. Quantification of SARS-CoV-2 *orf1* transcripts showed significant decline (~ 6.8 fold) in shHDAC6-transfected cells compared to mock transfected cells, whereas, HDAC6-overexpressing cells showed ~ 4-fold increase

Mukherjee *et al. Virology Journal*   (2024) 21:186

Page 5 of 16

Table 2 List of antibodies used in the study

Antibody/Reagent name	Species (IgG) specificity	Catalogue number	Manufacturer
Primary antibodies			
SARS- CoV-2 Spike	Rabbit	40591-T62	Sino Biological
SARS-CoV-2 NSP13	Rabbit	PA5-120711	Thermo Scientific
SARS-CoV-2 Nucleocapsid	Rabbit	40143-R001	Sino Biological
SARS-CoV-2 Nucleocapsid	Mouse	MA5-29981	Thermo Scientific
HDAC6	Mouse	ab56926	Abcam
HDAC6	Rabbit	ab133493	Abcam
HDAC6	Rabbit	7558S	Cell signaling
G3BP1	Mouse	Ab56574	Abcam
G3BP1	Mouse	Sc-365338	Santa Cruz Biotechnology
TIA-1	Rabbit	A6237	ABclonal
Acetyl-α-Tubulin	Rabbit	5335S	Cell signaling
HSP90	Rabbit	4875	Cell signaling
Ac-lysine Antibody	Mouse	sc-32268	Santa Cruz Biotechnology
PABP	Mouse	sc-32318	Santa Cruz Biotechnology
GAPDH (HRP conjugate)	Mouse	sc-25778	Santa Cruz Biotechnology
K48-linkage Specific Polyubiquitin Antibody	Rabbit	4289	Cell signaling
Phosphoserine Antibody	Mouse	sc81514	Santa Cruz Biotechnology
Beta Actin Antibody (C4) HRP	Mouse	Sc-47778	Santa Cruz Biotechnology
Secondary antibodies			
Anti-Rabbit IgG Rhodamine conjugate	Goat	31670	Thermo Scientific
Anti-Mouse IgG Rhodamine conjugate	Goat	31660	Thermo Scientific
Anti-Rabbit IgG DyLight™ 488 conjugate	Goat	35552	Thermo Scientific
Anti-Mouse IgG DyLight™ 488 conjugate	Goat	35502	Thermo Scientific
Anti-Rabbit IgG HRP conjugate	Goat	31460	Thermo Scientific
Anti-Mouse IgG HRP conjugate	Goat	31430	Thermo Scientific

in SARS-CoV-2 RNA. Quantification of *hdac6* mRNA confirmed efficient knockdown of *hdac6* in shHDAC6-transfected cells (Fig. 2A). Overall, the result suggested a proviral role of HDAC6 during SARS-CoV-2 infection. In the same set of experiments, expression of viral proteins was also assessed by immunoblotting. Results revealed reduced expression of SARS-COV-2 proteins non-structural protein 13 (NSP13) and Spike (S) in HDAC6 knockdown cells whereas ectopic expression of HDAC6 led to increased level of respective proteins which further established proviral role of HDAC6 in regulating SARS-CoV-2 infection (Fig. 2B).

To examine the mechanism by which HDAC6 may exert its proviral role, we inhibited the deacetylase activity of HDAC6 using increasing doses of selective deacetylase activity inhibitor, tubacin (0.5–2.5 μM). Initially efficiency of tubacin (0.5–5 μM) was tested in A549 cells by assessing its impact on its substrate α-tubulin via western blot using acetylated α-tubulin-specific antibody. Acetylation of α-tubulin was found to increase significantly upon tubacin treatment showing maximum effect at the doses of 2.5 and 5 μM (Supplementary Fig. 2)

which confirmed effective inhibition of HDAC6 activity by tubacin. In SARS-CoV-2-infected A549 cells, tubacin effectively reduced NSP13 and S protein expression in a dose-dependent manner showing maximum efficacy at 2.5 μM (Fig. 2C). Consistent to the viral protein expression data, SARS-CoV-2 *orf1a* transcript was also found to be significantly downregulated in SARS-CoV-2-infected A549 cells in presence of 1–2.5 μM tubacin (~6-fold reduction at 1 μM tubacin & ~13-fold reduction at 2.5 μM tubacin) (Fig. 2D). In addition, overexpression of HDAC6 catalytic mutant plasmid pcDNA-HDAC6.DC-FLAG failed to induce the expression of viral transcripts compared to pcDNA-HDAC6-FLAG overexpressing cells which further emphasizes the role of HDAC6 deacetylase activity in positively regulating SARS-CoV-2 infection (Fig. 2E). Altogether, these findings suggest that HDAC6 facilitates SARS-CoV-2 infection.

We further went on to decipher the effect of deacetylase activity of HDAC6 on the production of mature SARS-CoV-2 virus particles. Tubacin-treated (1–2.5 μM) and SARS-CoV-2-infected A549 cell supernatants were collected at different time points post
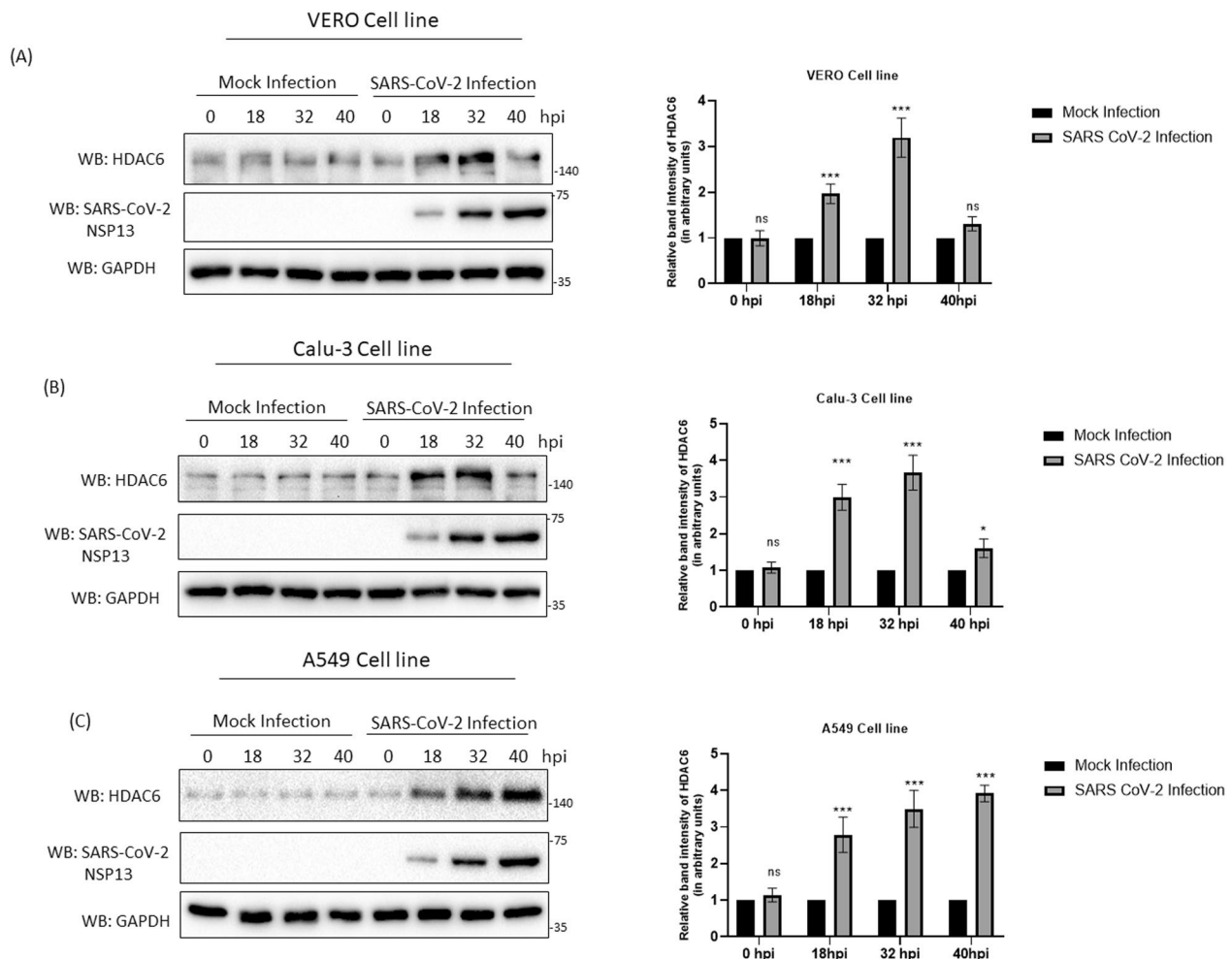
Fig. 1 SARS-CoV-2 infection leads to increased expression of HDAC6. **A** VERO E6 cells (at a MOI of 1), **B** Calu-3 cells (at a MOI of 1) and **C** A549 cell (at a MOI of 2) infected with SARS-CoV-2 or kept mock-infected were harvested at indicated time post-infection (18, 32, and 40 hpi) and cellular lysates were prepared. Lysates were run on SDS-PAGE followed by western blot analysis using anti-HDAC6 antibody. GAPDH and NSP13 were used as internal loading control and SARS-CoV-2 infection marker respectively

infection (24–72 hpi) followed by plaque assay. Tubacin treatment at a concentration of 1 μM and 2.5 μM resulted in significant reduction in viral progeny yield (Fig. 2F). To further assess the impact of HDAC6 deacetylase activity on the generation of mature viral particles, we collected supernatants from SARS-CoV-2-infected (24–72 hpi) A549 cells transfected with either pFLAG HDAC6, pcDNA-HDAC6.DC-FLAG, or shHDAC6. Subsequently, we performed plaque assay. Significant reduction in mature viral progeny production was observed in cells ectopically expressing catalytic deficient HDAC6 compared to wild type HDAC6-overexpressing cells (Fig. 2G), similar to the reduction observed during tubacin treatment (Fig. 2F). Additionally, cells transfected with shHDAC6 exhibited a significant reduction in viral particle production

compared to empty vector-transfected control cells (Fig. 2G).

Interaction between HDAC6 and G3BP1 is increased during SARS-CoV-2 infection

Next, we focused on investing the mechanism by which HDAC6 exerts its proviral role in regulating SARS-CoV-2 infection. HDAC6 has been identified as one of the major cytoplasmic tubulin deacetylase [18, 59]. Hence, we assessed the level of acetylated α-tubulin in A549 cells during SARS-CoV-2 infection at different time points via western blot. To our surprise, no significant change in the acetylation of α-tubulin was observed during SARS-CoV-2 infection (Fig. 3A). Next we analysed the acetylated α-tubulin levels in VERO and Calu-3 cells during the course of SARS-CoV-2 infection and we did not observe any significant change in the expression level of
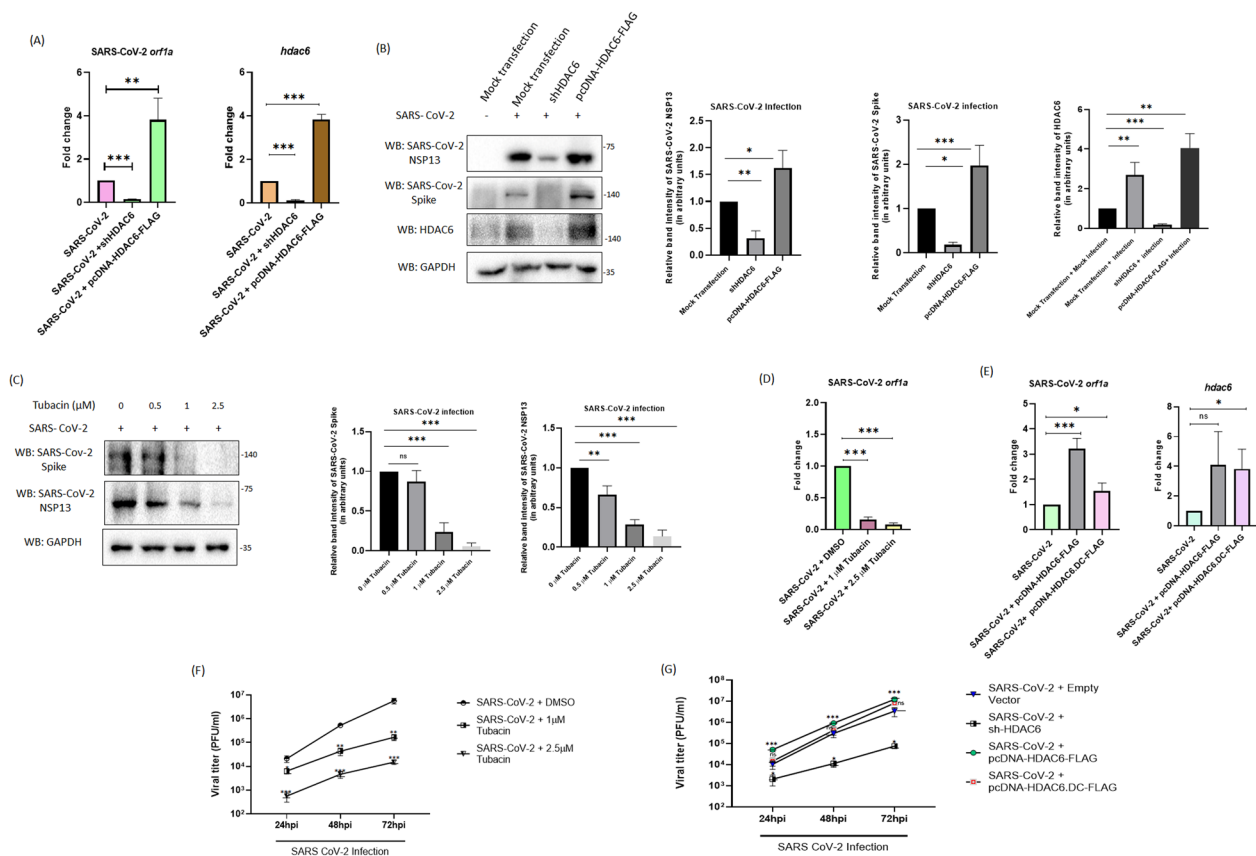
Mukherjee *et al. Virology Journal* (2024) 21:186

Page 7 of 16

Fig. 2 Inhibition of HDAC6 resulted in reduction of SARS CoV-2 replication. **A** A549 cells were either transfected with shHDAC6 or pcDNA-HDAC6-FLAG followed by SARS-CoV-2 infection (at a MOI = 1). Total RNA was isolated after 24 h of infection followed by qRT-PCR using SARS-CoV-2 *orf1a, hdac6* and *gapdh*-specific primers. Data represent means ± SD of three independent experiments. ***$p \leq$ .001, unpaired t-test and **$p \leq$ .01, unpaired t-test. **B** Protein was extracted from SARS-CoV-2 infected cells at 24 hpi (MOI = 1) ectopically expressing shHDAC6 or pcDNA-HDAC6-FLAG. S, NSP13 and HDAC6 expression levels were analysed via western blotting. **C** SARS-CoV-2 infected (24 hpi) A549 cells were treated with increasing doses of tubacin (0–2.5 μM). Cellular extracts were subjected to immunoblot to analyse levels of S and NSP13. GAPDH was used as internal loading control. **D** Total RNA was isolated from tubacin treated SARS-CoV-2 infected cells (MOI = 1) at 24 hpi followed by qRT-PCR using SARS-CoV-2 *orf1a* and *gapdh* specific primers. Data represent means ± SD of three independent experiments. ***$p \leq$ .001, unpaired t-test and **$p \leq$ .01, unpaired t-test. **E** A549 cells were either transfected with empty vector or pcDNA-HDAC6-FLAG or pcDNA-HDAC6. DC-FLAG followed by SARS-CoV-2 infection (at a MOI = 0.5). Total RNA was isolated after 24 h of infection followed by qRT-PCR using SARS-CoV-2 *orf1a, hdac6* and *gapdh*-specific primers. Data represent means ± SD of three independent experiments. ***$p \leq 0.001$, unpaired t-test, *$p \leq 0.1$, unpaired t-test and ns = not significant, unpaired t-test. **F** A549 cells were infected with SARS-CoV-2 (MOI = 1) either in presence or absence of tubacin (1–2.5 μM) for 24, 48 and 72 h followed by plaque assay. Viral titers were measured as plaque forming units [log (pfu/ml)]. Data represent means ± SD of three independent experiments. **$p \leq$ .01, multiple t-tests,***$p \leq$ .001, multiple t-tests and ns = not significant, multiple t-tests. **G** A549 cells were either transfected with empty vector or shHDAC6 or pcDNA-HDAC6-FLAG or pcDNA-HDAC6.DC-FLAG followed by SARS-CoV-2 infection (at a MOI = 0.5) for 24, 48 and 72 h followed by plaque assay. Viral titers were measured as plaque forming units [log (pfu/ml)]. Data represent means ± SD of three independent experiments. ***$p \leq$ .001, multiple t-tests, *$p \leq 0.05$, multiple t-tests and ns = not significant, multiple t-tests

acetylated α -tubulin levels in Calu-3 cells. Mild decrease in the level of acetylated α-tubulin level was observed in VERO cells at 18 hpi which restored from 24 hpi (Supplementary Fig. 3A and B). Altogether the data suggests the involvement of α-tubulin-independent mechanisms in regulating SARS-CoV-2 infection during HDAC6 inhibition. In addition to α-tubulin, HDAC6 interacts and/or mediates deacetylation of an array of other non-histone proteins including Heat Shock protein 90 (HSP90),

cortactin and Ras GTPase-activating protein-binding protein 1 (G3BP1) [24, 58]. To investigate the association of HDAC6 with HSP90 and G3BP1, we performed co-immunoprecipitation assay during SARS-CoV-2 infection (18–32 hpi) using HDAC6-specific antibody. Immunoblot analysis of HDAC6 immunoprecipitates using anti-HSP90 antibody revealed no significant alteration in association between HDAC6 with HSP90 at different time post virus infection (Fig. 3B). Whereas, the
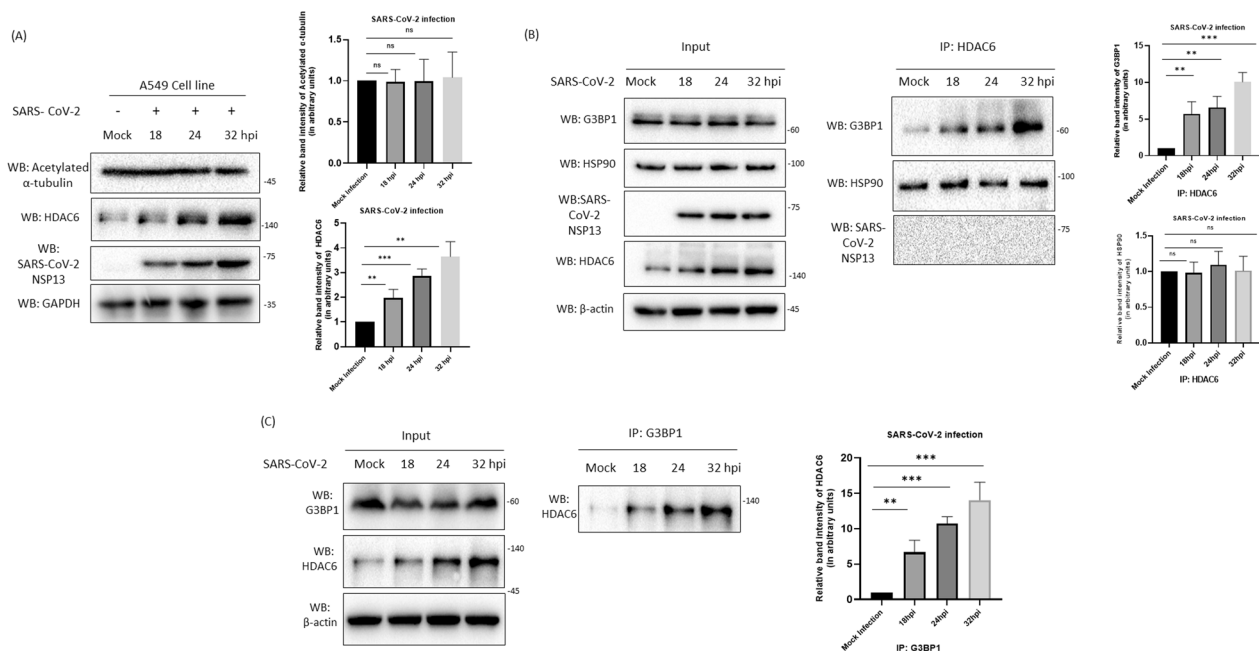
Mukherjee *et al. Virology Journal*   (2024) 21:186

Page 8 of 16

Fig. 3 Increased interaction between G3BP1 and HDAC6 during SARS-CoV-2 infection. **A** Cellular lysates from A549 cells either infected with SARS-CoV-2 at a MOI of 2 (18–32 hpi) or kept mock-infected were run on SDS-PAGE and protein level expression of acetylated α-tubulin, HDAC6 and NSP13 protein was analysed via western blotting. **B** SARS-CoV-2-infected (18–32 hpi) or mock-infected lysates were pulled down using HDAC6-specific antibody followed by western blot analysis of the immunoprecipitates by anti-G3BP1, anti-HSP90 and anti-NSP13 antibodies. Inputs were probed with anti-HSP90, anti-G3BP1, anti-HDAC6, anti-NSP13 and β-actin antibodies confirming protein expression. (**C**) Reciprocal co-immunoprecipitation analysis was carried out in SARS-CoV-2-infected (18–32 hpi) or mock-infected lysates; anti-G3BP1 was used for pull down and immunoblot analysis was performed with HDAC6-specific antibody. Inputs were probed with anti-G3BP1, anti-HDAC6 and β-actin antibodies

association between G3BP1 and HDAC6 was found to increase gradually with increasing time points post SARS-CoV-2 infection. As a control HDAC6 immunoprecipitate was also blotted for viral protein NSP13 and no interaction was found, suggesting that increased HDAC6 and G3BP1 interaction during SARS-CoV-2 infection is specific (Fig. 3B). Reciprocal co-immunoprecipitation assay using anti-G3BP1 antibody also corroborated increased interaction between HDAC6 and G3BP1 during SARS-CoV-2 infection in a time-dependent manner (Fig. 3C). Phosphorylation of G3BP1 at the serine 149 residue has been previously reported [26] to be critical for its interaction with HDAC6. Co-immunoprecipitation assay using phospho-serine specific antibody in A549 cells infected with SARS-CoV-2 followed by immunoblotting with G3BP1 revealed no significant change in serine phosphorylation of G3BP1 during SARS-CoV-2 infection (Supplementary Fig. 4).

SARS-CoV-2 N protein engages in interaction with HDAC6
SARS-CoV-2 N protein has been previously reported to interact with and sequester G3BP1 during infection to attenuate SG formation [29, 62]. Hence, we looked into the possibility of interaction between HDAC6 and N

protein. Lysates prepared from SARS-CoV-2-infected A549 cells were pulled down with anti-HDAC6 antibody. Immunoprecipitates were probed using N protein-specific antibody. Presence of N protein in HDAC6 immunoprecipitate suggested interaction between HDAC6 and N protein (Fig. 4A). N protein is one of the most abundant protein of SARS-CoV-2 [11], hence to dismiss the possibility of non-specific pull down of N protein due to high abundance, we probed the membrane with another highly expressed protein of SARS-CoV-2, namely Spike protein. Absence of Spike protein in the immunoprecipitates of HDAC6 confirmed specific interaction between HDAC6 and SARS-CoV-2 N protein (Fig. 4A). Co-immunoprecipitation assay from A549 cells overexpressing pcDNA3.1-N protein using anti-HDAC6 antibody also showed presence of N protein in the immunoprecipitate when probed with anti-N protein antibody. Interestingly, input lanes of pcDNA3.1-N-transfected lysate showed increased expression of HDAC6 compared to mock-transfected lysate (Fig. 4B). Reciprocal co-immunoprecipitation assay using anti-N protein antibody during SARS-CoV-2 N protein overexpression also validated the interaction between HDAC6 and N protein. In consistence with the previous observation, input lanes of
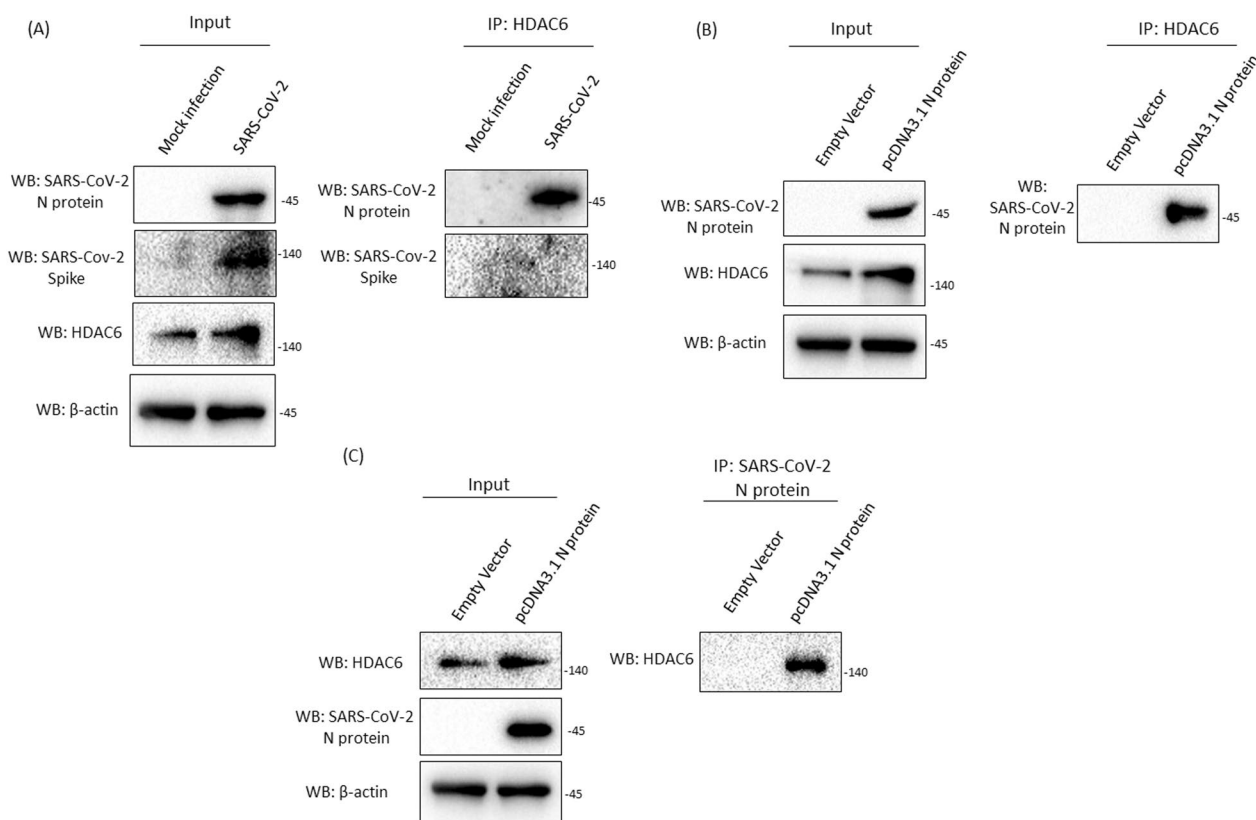
Fig. 4 SARS-CoV-2 N Protein interacts with HDAC6. **A** Cellular lysates from SARS-CoV-2-infected or mock-infected A549 cells were co-immunoprecipitated with anti-HDAC6 antibody. Western blot analysis was performed to check the expression of N protein and SARS-CoV-2 Spike protein within the HDAC6 immunoprecipitates. Inputs were probed with anti-HDAC6, anti-N and anti-Spike antibodies confirming protein expression. **B** A549 cells were either transfected with pcDNA3.1-N plasmid or empty vector followed by immunoprecipitation with anti-HDAC6 antibody. Immunoblot analysis was performed with anti-N protein and anti-HDAC6 antibody. **C** Reciprocal co-immunoprecipitation assay from A549 cells either transfected with pcDNA3.1-N or empty vector using anti-N protein antibody was performed. Immunoprecipitates were analysed for the expression of HDAC6 and N protein. Inputs were probed with anti-HDAC6, anti-N and anti-β-actin antibodies confirming protein expression

ectopically expressing N protein again showed elevated level of HDAC6 in comparison to mock-transfected control (Fig. 4C).

SARS-CoV-2 N protein triggers the expression of HDAC6 via increasing its stability

In the preceding section, increased level of HDAC6 was observed in input lysates of N protein-expressing cells (Fig. 4A and B), hence, we hypothesized that HDAC6 expression may be regulated by N protein. To confirm, A549 cells were transfected with increasing concentration of pcDNA3.1-N (1–3 µg) and lysates were analysed for HDAC6 expression via immunoblot analysis. Result showed a dose-dependent positive correlation between the amount of transfected pcDNA3.1-N and the induction of HDAC6 expression suggesting that N protein alone is sufficient to induce protein level expression of HDAC6 during SARS-CoV-2 infection (Fig. 5A). Moreover, the in vitro ectopic expression of

either SARS-CoV-2 Spike protein or NSP13 failed to induce HDAC6 expression. This finding further corroborates specificity of SARS-CoV-2 N protein in regulation of HDAC6 expression (Supplementary Fig. 5). In line with the infection scenario, increased association between HDAC6 and G3BP1 was also found in cells ectopically expressing SARS-CoV-2 N protein which further confirmed involvement of N protein in regulating HDAC6 expression during infection (Fig. 5B). Similar to infection scenario, quantitative real-time PCR from pcDNA3.1-N-transfected A549 cells showed no significant change in the expression level of *hdac6* RNA when normalized to *gapdh* (Fig. 5C). The result suggests that SARS-CoV-2 N protein regulates expression HDAC6 post-transcriptionally. To analyse whether HDAC6 expression is regulated at the translation level, Cycloheximide (CHX) chase assay was performed in cells overexpressing N protein. Briefly, A549 cells were transfected with either empty vector or pcDNA3.1-N
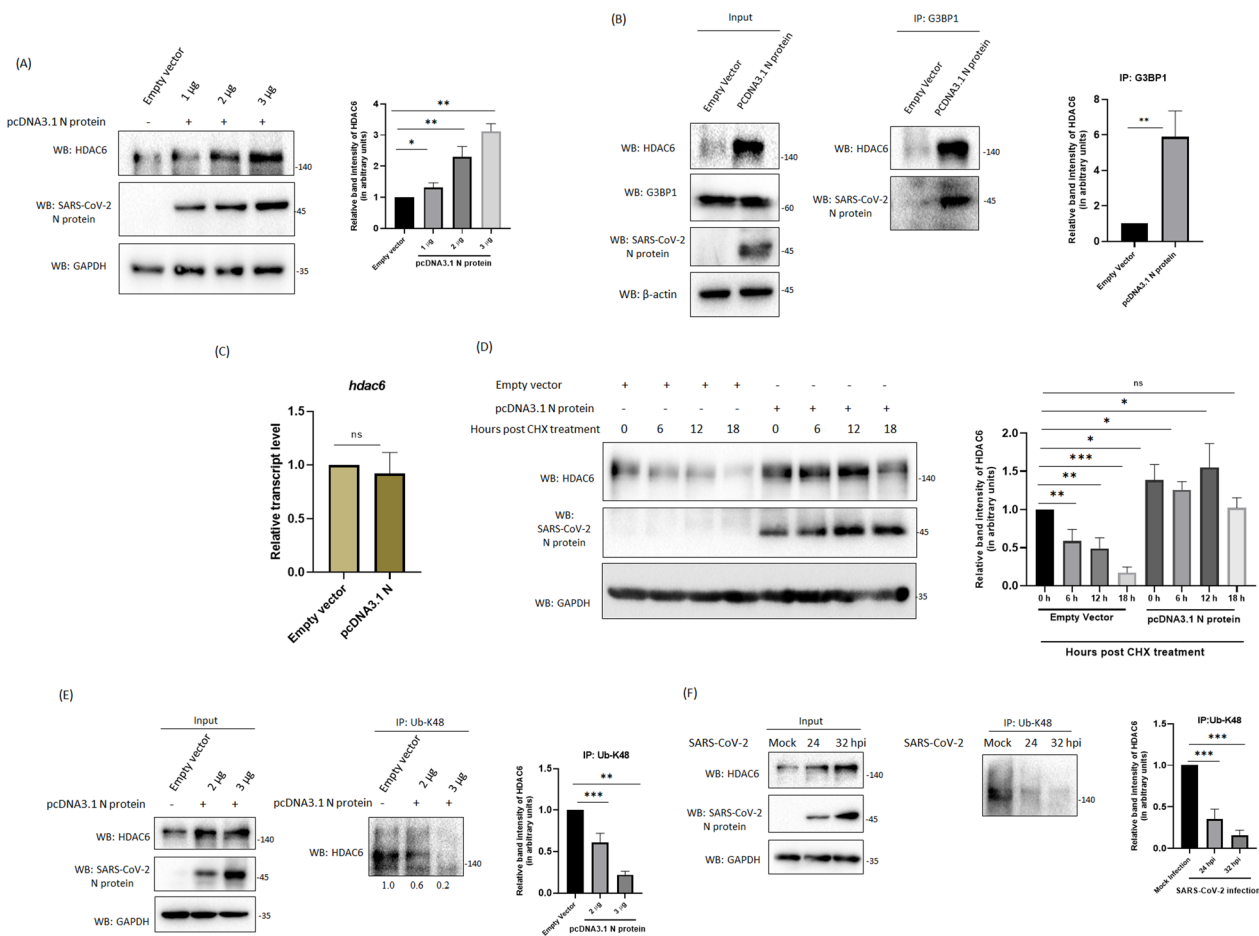
Mukherjee *et al. Virology Journal*   (2024) 21:186

Page 10 of 16

Fig. 5 SARS-CoV-2 N Protein induces expression of HDAC6. **A** Cellular lysates were prepared from A549 cells either transfected with increasing concentration of pcDNA3.1-N (1–3 μg) or transfected with empty pcDNA3.1 vector. Expression of HDAC6, N protein and GAPDH was analysed via western blotting. **B** Co-immunoprecipitation analysis was performed in A549 cells either pcDNA3.1-N protein-transfected or empty vector-transfected A549 cells using anti-G3BP1 antibody and immunoblot analysis was performed using HDAC6 and N protein-specific antibodies. **C** Total RNA was isolated from A549 cells either transfected with empty vector or pcDNA3.1-N protein followed by qRT-PCR using *hdac6* and *gapdh*-specific primers. ns = not significant, unpaired t-test. **D** A549 cells were either transfected with empty vector or pcDNA3.1 N protein followed by CHX treatment at 18 h post-transfection. Cells were harvested at indicated time post-CHX treatment (0, 6, 12, 18) and HDAC6, SARS-CoV-2 N protein and GAPDH expressions were analysed via immunoblotting. **E** A549 cells were either transfected with pcDNA3.1-N protein or empty vector followed by immunoprecipitation with anti-K48-ubiquitin antibody. Immunoblot analysis was performed with anti-HDAC6 antibody. **F** SARS-CoV-2-infected (24–32 hpi) or mock-infected lysates were pulled down using with anti-K48-ubiquitin antibody. Immunoblot analysis was performed with anti-HDAC6 antibody

protein followed by CHX (10 μM) treatment at 18 h post-transfection. Cells were harvested at indicated time points (0, 6, 12, 18 h). Cells ectopically expressing empty vector showed gradual decrease in the expression level of HDAC6 following CHX treatment. A549 cells expressing N protein did not show significant alteration in the expression level of HDAC6 up to 18 h post-CHX treatment, thus suggesting that N protein-mediated induction in HDAC6 protein level was not due to accelerated translation (Fig. 5D). Next, we evaluated the K48-ubiquitination status of HADC6

in A549 cells ectopically expressing pcDNA3.1 N protein. Co-immunoprecipitation using K48-ubiquitin-specific antibody showed reduced K48-ubiquitylation of HDAC6 in N protein-overexpressing cells compared to empty vector-transfected cells (Fig. 5E). Similar reduction in K48-ubiquitylation of HDAC6 was also observed during SARS-CoV-2 infection (Fig. 5F). Collectively, these findings suggest that the SARS-CoV-2 N protein enhances the stability of HDAC6 during infection via reducing its proteasomal degradation, thereby leading to elevated levels of HDAC6 protein.

HDAC6-mediated deacetylation of SARS-CoV-2 N protein is crucial for its interaction with SG protein G3BP1

Interaction between G3BP1 and SARS-CoV-2 N protein has been established, thus the association of HDAC6 with N protein may be merely a consequence of this interaction. Hence we went on to find out the functional relevance of the presence of HDAC6 along with G3BP1 in the immunoprecipitates of SARS-CoV-2 N protein. A549 cells were co-transfected with pcDNA3.1-N along with either shHDAC6 plasmid or pcDNA-HDAC6-FLAG followed by immunoprecipitation with G3BP1 antibody. Western blot analysis of G3BP1 immunoprecipitates revealed significantly reduced level of N protein in HDAC6 knocked down cells whereas high amount of N protein was found in HDAC6-overexpressing cells. This suggested that HDAC6 umpires the interaction between G3BP1 and SARS-CoV-2 N protein (Fig. 6A). Next, we assessed the interaction between G3BP1 and N protein either in presence or absence of tubacin. Interestingly, the association between SARS-CoV-2 N protein and G3BP1 was found to decrease in presence of tubacin (2.5 μM) compared to only DMSO treatment suggesting the role of deacetylase activity of HDAC6 for mediating the association between SARS-CoV-2 N protein and G3BP1 during SARS-CoV-2 infection (Fig. 6B). The positive regulatory role of HDAC6 deacetylase activity in the association between G3BP1 and N protein was further established when catalytic mutant of HDAC6 failed to enhance their association in A549 cells, in contrast to the

cells overexpressing the wild-type HDAC6 (Fig. 6C). This rules out the possibility of any off target activity of tubacin that could have interrupted the interaction between SARS-CoV-2 N protein and G3BP1.

Next, we assessed the acetylation status of N protein and G3BP1 either in presence or absence of tubacin. To check this, we performed co-immunoprecipitation assay using Ac-Lys-specific antibody in pcDNA-N protein-overexpressing cells either treated with tubacin (2.5 μM) or left untreated, followed by western blotting to analyse the levels of N protein and G3BP1. To our surprise, acetylation of SARS-CoV-2 N protein was found to increase significantly in presence of tubacin (Fig. 6D). Similar increased acetylation of N protein was observed in HDAC6-depleted cells (Supplementary Fig. 6), suggesting that HDAC6 deacetylates N protein during infection. Collectively, the results suggest that HDAC6 promotes deacetylation of SARS-CoV-2 N protein which positively modulates the N protein and G3BP1 interaction (Fig. 6D and Supplementary Fig. 6). In contrast, acetylation status of G3BP1 remained unaltered during HDAC6 inhibition as well as during shRNA-mediated knock down of HDAC6 (Fig. 6D and Supplementary Fig. 6).

Induction of HDAC6 expression during SARS-CoV-2 infection facilitates stress granule disruption

Association between G3BP1 and SARS-CoV-2 N protein is known to impair cellular SG formation [62]. Hence, we analysed the effect of inhibition of HDAC6 on the
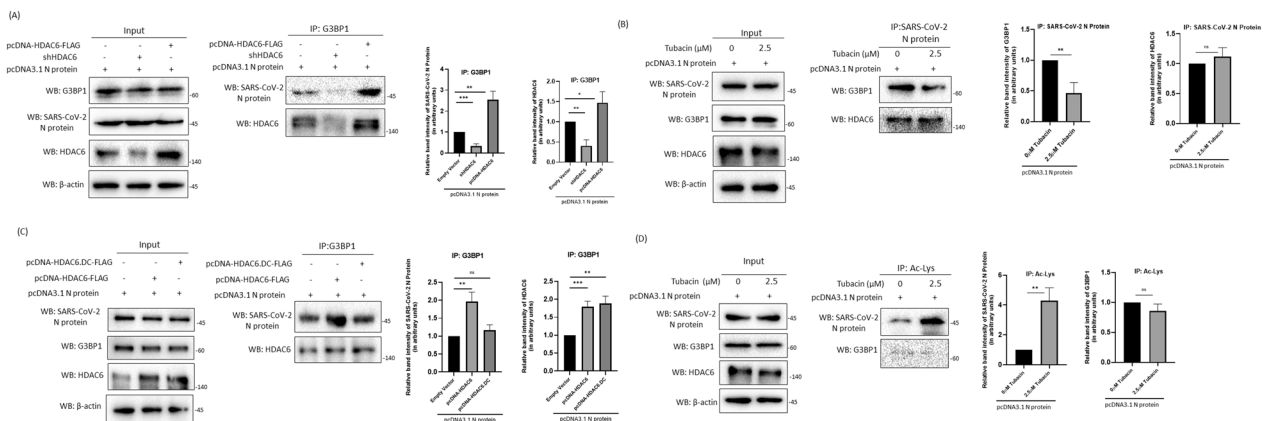

Fig. 6 HDAC6 mediates interaction between G3BP1 and SARS-CoV-2 N protein. **A** A549 cells were transfected with pcDNA3.1-N and co-transfected with either pcDNA-HDAC6-FLAG or shHDAC6 were analysed by co-immunoprecipitation by using anti-G3BP1 antibody. Immunoprecipitates were subjected to western blot analysis using HDAC6 and SARS-CoV-2 N protein-specific antibody. **B** A549 cells transfected with pcDNA3.1-N plasmid either in presence or absence of tubacin (2.5 μM), followed by co-immunoprecipitation of cellular lysates with anti-SARS-CoV-2 N protein antibody. Immunoblot analysis was performed to check the expression of G3BP1 and HDAC6. **C** A549 cells were transfected with pcDNA3.1-N and co-transfected with either pcDNA-HDAC6-FLAG or pcDNA-HDAC6.DC-FLAG. Cellular lysates were subjected to co-immunoprecipitation using anti-G3BP1 antibody. Western blot analysis was performed using SARS-CoV-2 N protein and HDAC6-specific antibodies. Input lanes were probed with anti-G3BP1, anti-HDAC6 and anti-SARS-CoV-2 N antibodies. **D** A549 cells transfected with pcDNA3.1-N and either treated with tubacin (2.5 μM) or treated with DMSO. Cell lysates were subjected to immunoprecipitation using anti-Ac-Lys antibody. Western blot was performed using G3BP1 and HDAC6-specific antibodies

Mukherjee *et al. Virology Journal*   (2024) 21:186

Page 12 of 16

status of cellular SGs during ectopic expression of N protein. Cell lysates were prepared from sodium arsenite (NaAsO$_2$)-treated, pcDNA3.1-N protein-overexpressing A549 cells that were either treated with tubacin or were knocked down using shHDAC6. Cellular extracts were then subjected to immunoprecipitation using anti-TIA-1 antibody, a well-known component of SG. Western blot analysis of the TIA-1 immunoprecipitates revealed significantly increased association between SG components TIA-1, G3BP1 and PABP in HDAC6-knocked down cells compared to control cells during N protein overexpression. Similar pattern of increased association between TIA-1, G3BP1 and PABP was also observed during tubacin treatment (2.5 μM) (Fig. 7A). Interestingly, sodium arsenite, a known oxidative stressor also failed to induce SG formation in cells overexpressing N protein. Overall, the data suggested that assemblage of different SG components in N protein-overexpressing cells is inhibited by HDAC6. This observation was further validated via immunofluorescence microscopy in sodium arsenite-treated cells using G3BP1 as marker. Oxidative stress-induced bonafide SGs were found in mock-transfected control cells. Ectopic expression of N protein resulted in complete attenuation of NaAsO$_2$-induced SG formation in A549 cells (Fig. 7B), whereas tubacin treatment restored SG formation in N protein-overexpressing cells. Overall the results suggest that induction of HDAC6 during SARS-CoV-2 infection negatively impacts cellular SG formation (Fig. 7B).

Discussion

The role of HDAC6 in modulating virus infection remains enigmatic as it displays both pro- and antiviral effects. Antiviral role of HDAC6 is multifaceted ranging from upregulation of IFNβ production during Sendai virus infection [38] to modulation of the RIG-I-mediated antiviral sensing pathway [9]. Whereas proviral roles include positive regulation of HCV replication [25], facilitation of KSHV reactivation [46], and acting as granulophagic cargo to evade antiviral immune response during coxsackievirus infection [61]. As SARS-CoV-2 has shown wide range of immune response modulation in the host, the present study was undertaken to decipher possible involvement of HDAC6 in the regulation of SARS-CoV-2 infection. SARS-CoV-2 infection was found to result in gradual increase in the expression of HDAC6 protein in a three different cell lines including VERO, Calu-3 and A549 (Fig. 1).

Next we observed reduced expression of SARS-CoV-2 viral genes in HDAC6-knocked down cells and ectopic
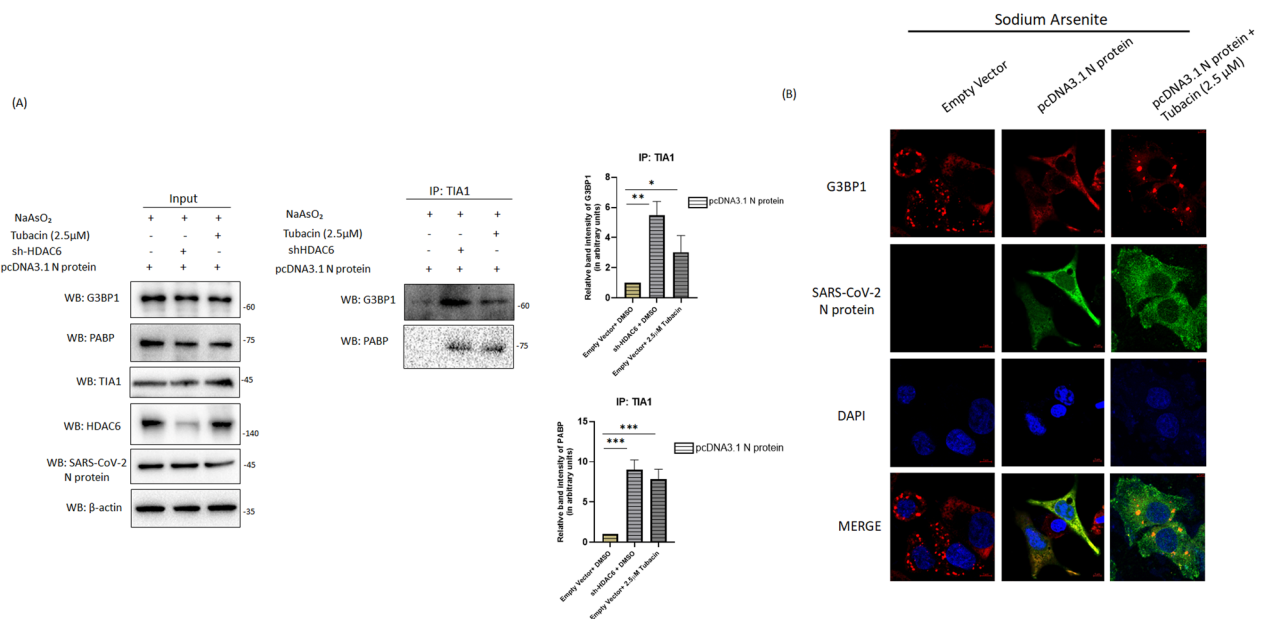

Fig. 7 Induction of HDAC6 expression during SARS-CoV-2 infection facilities disruption of Stress Granules. **A** A549 cells were transfected with pcDNA3.1-N protein and/or co-transfected with shHDAC6 followed by either tubacin (2.5 μM) or DMSO treatment. Cells were treated with NaAsO$_2$ 1 h before harvesting. Co-immunoprecipitation was performed from the cellular lysates in using anti-TIA-1 antibody. Western blot was performed using PABP, N protein, G3BP1, HDAC6 and TIA-1-specific antibodies. **B** A549 cells were either transfected with pcDNA3.1-N protein or empty vector and either treated with tubacin (2.5 μM) or left untreated. 1 h before fixation cells were treated with NaAsO$_2$ followed by permeabilization and staining with anti-G3BP1 and anti-N protein primary antibody. Secondary staining was performed with Rhodamine-conjugated anti-mouse (for G3BP1) and DyLight™ 488-conjugated anti-rabbit (for N protein) secondary antibodies. DAPI was used for mounting. Imaging was done with a confocal microscope (63× oil immersion) and scale bar was set at 5 μm

Mukherjee *et al. Virology Journal*   (2024) 21:186

Page 13 of 16

expression of HDAC6 resulted in increased expression of viral genes corroborating the proviral role of HDAC6 (Fig. 2A and B). Inhibiting HDAC6's deacetylase activity using a small molecule inhibitor, tubacin [32] led to a dose-dependent decrease in SARS-CoV-2 replication (Fig. 2C, D and F). Furthermore, ectopic expression of the catalytic mutant plasmid pcDNA-HDAC6.DC-FLAG failed to promote SARS-CoV-2 replication compared to pFLAG HDAC6 expressing cells highlighting the indispensability of HDAC6's deacetylation activity during SARS-CoV-2 infection (Fig. 2E and G). Altogether, SARS-CoV-2 growth kinetics data from HDAC6 depleted and overexpressing and Tubacin treated cells (Fig. 2F and G) establishes the proviral role of HDAC6 in regulating SARS-CoV-2 infection.

HDAC6 exerts its antiviral role during IAV infection by inducing deacetylation of microtubules which in turn results in reduced trafficking of viral components to plasma membrane [19]. However, we did not observe any significant alteration in the expression level of acetylated α-tubulin during the course of SARS-CoV-2 infection in A549, Calu-3 and VERO cells (Fig. 3A and Supplementary Fig. 3). Interaction between HDAC6 and HSP90, which is another cytoplasmic target of HDAC6, also remained unchanged during the course of SARS-CoV-2 infection (Fig. 3B). This finding eliminates the likelihood of HSP90-mediated regulation of SARS-CoV-2 infection. Nevertheless, co-immunoprecipitation experiments confirmed substantial increase in interaction between HDAC6 and G3BP1 in time-dependent manner during SARS-CoV-2 infection (Fig. 3B, C).

Previous studies have shown that HDAC6 is a critical component for efficient formation of G3BP1-positive SGs [26, 52]. Interestingly, SARS-CoV-2 N protein impairs cellular SG formation via its interaction with SG protein G3BP1. SARS-CoV-2 N protein shifts the cellular RNA binding preferences of G3BP1, sequestering it away from its wild type targets which in turn negatively impacts SG formation [29, 36, 62]. These findings pose a sharp contrast to our observation of increased interaction between HDAC6 and G3BP1 which is suggestive of accelerated SG formation. In addition, interaction between HDAC6 and N protein in SARS-CoV-2-infected cells as well as in cells ectopically expressing SARS-CoV-2 N protein was observed (Fig. 4A, B and C). Moreover, N protein itself was found to be sufficient to induce HDAC6 expression in a dose-dependent manner (Fig. 5A). Co-immunoprecipitation experiments revealed substantial increase in interaction between HDAC6 and G3BP1 during SARS-CoV-2 N protein overexpression compared to mock-transfected cells. Altogether these findings suggest that N protein alone is capable to induce HDAC6 expression and its interaction with G3BP1 (Fig. 5B). The addition of

K48-linked polyubiquitin chains to proteins serves as a universal signal for degradation by the proteasome [43]. The decreased association of HDAC6 with K48-linked polyubiquitin during infection and SARS-CoV-2 N protein overexpression suggests that the N protein increases the stability of HDAC6 (Fig. 5E, F). Furthermore, depletion of HDAC6 using either shRNA or inhibiting its deacetylation activity resulted in decreased association between G3BP1 and N protein, emphasizing the pivotal role of HDAC6 in interacting with N protein (Fig. 6A–C). HDAC6-mediated K376 deacetylation of G3BP1 has been reported to be crucial for RNA binding and thus promotes the formation of cellular SGs [14]. In contrast, HDAC6-mediated deacetylation of Protein Arginine Methyltransferase 5 (PRMT5) has been reported to alter its methyltransferase activity, leading to reduced dimethylation of G3BP1 [15]. Additionally, the deacetylation of the cellular RNA helicase DDX3X via HDAC6 is necessary for SG maturation [42]. Acetylation of the N protein of SARS-CoV and SARS-CoV-2 has been previously shown to be promoted by two human histone acetyltransferases namely, P300/CBP-associated factor (PCAF) and general control nonderepressible 5 (GCN5) [17], which led us to hypothesize that HDAC6-mediated deacetylation of either G3BP1 or N protein might influence their association. Indeed, either shRNA-mediated depletion of HDAC6 protein level or inhibition of deacetylase activity of HDAC6 reveals remarkably increased acetylation of SARS-CoV-2 N protein, whereas acetylation status of G3BP1 remained unaltered (Fig. 6D and Supplementary Fig. 6). Cumulatively, these findings suggest that HDAC6 induces deacetylation of N protein which might be crucial for its association of G3BP1. Furthermore, we did not observe any change in the serine phosphorylation level of G3BP1 during SARS CoV-2 infection (Supplementary Fig. 4), which according to [26] is essential for regulating its association with HDAC6 [26]. Therefore, we hypothesize that the increased association between HDAC6 and G3BP1 observed during infection is independent of the phosphorylation status of G3BP1 and likely due to the presence of HDAC6 within the G3BP1 and N protein interaction complex.

SGs act as a signaling hub that plays a critical role in type I interferon responses during RNA virus infections [55]. Hence viruses evolved diverse strategies to combat SG-mediated stress response. Many viruses induce SG formation in cells, either through eIF2α phosphorylation-dependent or -independent mechanisms [34, 39]. Typically, SGs dissipate at later stages of infection despite the continued phosphorylation of eIF2α [34]. Furthermore, external stressors like sodium arsenite fail to induce SGs in cells infected with many viruses, suggesting that these viruses can uncouple stress signals from SG formation
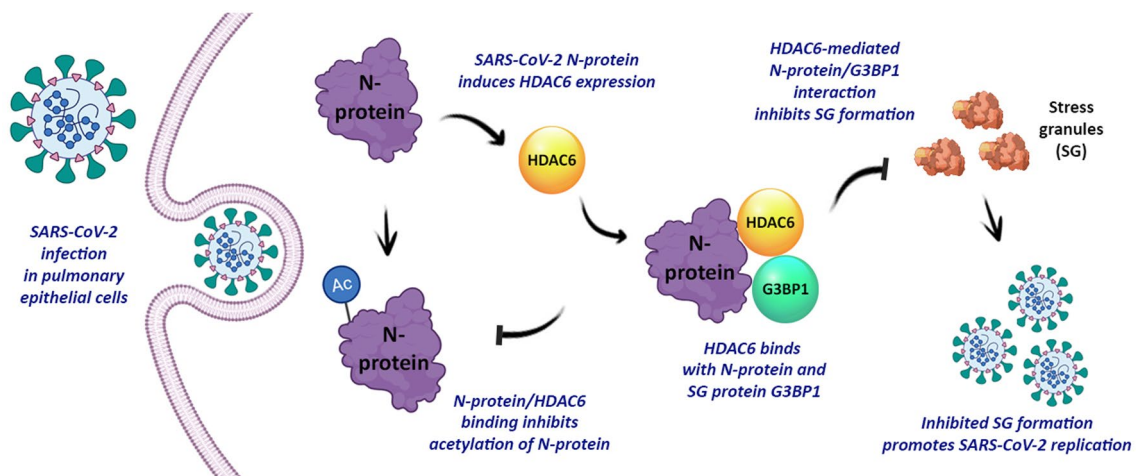
Mukherjee *et al. Virology Journal*   (2024) 21:186

Page 14 of 16

Fig. 8 Schematic representation showing crosstalk between HDAC6 and SARS-CoV-2 infection. SARS-CoV-2 N protein interacts with and induces the expression of HDAC6. Subsequently, HDAC6 promotes the deacetylation of the N protein, which facilitates its association with G3BP1, leading to the disruption of cellular stress granules

[20, 22, 50, 51]. SARS CoV-2 infection also inhibits cellular SG formation to promote its own replication [23, 30, 31, 36, 63]. In the present study we observed inhibitory effect of HADC6 in assemblage of different SG components namely TIA-1, PABP and G3BP1 in cells overexpressing N protein (Fig. 7A), suggesting that induction of HDAC6 might facilitate SG disruption during SARS-CoV-2 infection. This assumption was confirmed when sodium arsenite-induced distinct SGs reappeared in N protein-expressing cells following tubacin treatment (Fig. 7B). These results are in sharp contrast to most of the existing studies linking SG formation with HDAC6 which demonstrated that a variety of cellular stressors, including arsenite stress, heat shock, CCPP, and UV exposure trigger SG formation through the interactions of HDAC6 with microtubules, motor proteins, and SG components such as G3BP. The ability of HDAC6 to bind ubiquitinated proteins and dynein motors facilitates the transport of SGs along microtubules, further emphasizing its role in SG dynamics [14, 26]. Interestingly, Coxsackievirus A16, another enterovirus induces degradation of SGs using HDAC6 as a novel cargo for autophagic clearance of stress granules, thus disrupting SGs [61]. This finding aligns with our observation of the inhibitory role of HDAC6 on stress granules during SARS-CoV-2 infection.

Conclusion

The present study underscores an efficient strategy employed by SARS-CoV-2 to antagonize the formation of cellular SGs which positively aids in unhindered viral replication. SARS-CoV-2 N protein was found to promote its own deacetylation via inducing HDAC6 expression which is critical for its association with SG protein G3BP1 to prevent SG formation (Fig. 8). Though this is the first report on proviral role of HDAC6 in SARS-CoV-2 life cycle via deacetylation of N protein, further investigations are warranted to delineate other pathways which may be impacted due to HDAC6 mediated deacetylation during SARS-CoV-2 replication and propagation.

Supplementary Information

Supplementary Material 1.

Mukherjee *et al. Virology Journal*　　(2024) 21:186

Page 15 of 16

Declarations

Ethics approval and consent to participate
The study was approved by the institutional Biosafety committee. SARS-CoV-2 was isolated as a part of establishment of ICMR-COVID-19 biorepositories (Approval No. A-1/2020-IEC). Consent to participate is not applicable for the present study.

Consent for publication
Not applicable.

Competing interests
The authors declare no competing interests.

References
1. Agrawal P, Sambaturu N, Olgun G, Hannenhalli S. A path-based analysis of infected cell line and COVID-19 patient transcriptome reveals novel potential targets and drugs against SARS-CoV-2. Front Immunol. 2022;13:918817.
2. Ashour HM, Elkhatib WF, Rahman MM, Elshabrawy HA. Insights into the recent 2019 novel coronavirus (SARS-CoV-2) in light of past human coronavirus outbreaks. Pathogens. 2020;9(3):186.
3. Baer A, Kehn-Hall K. Viral concentration determination through plaque assays: using traditional and novel overlay systems. J Vis Exp. 2014;93:e52065. https://doi.org/10.3791/52065.PMID:25407402;PMCID:PMC4255882.
4. Banerjee I, Miyake Y, Nobs SP, Schneider C, Horvath P, Kopf M, Matthias P, Helenius A, Yamauchi Y. Influenza A virus uses the aggresome processing machinery for host cell entry. Science. 2014;346(6208):473–7.
5. Bayati A, Kumar R, Francis V, McPherson PS. SARS-CoV-2 infects cells after viral entry via clathrin-mediated endocytosis. J Biol Chem. 2021;296:100306.
6. Brant AC, Tian W, Majerciak V, Yang W, Zheng ZM. SARS-CoV-2: from its discovery to genome structure, transcription, and replication. Cell Biosci. 2021;11(1):1–17.
7. Chen F, Zhang Y, Sucgang R, Ramani S, Corry D, Kheradmand F, Creighton CJ. Meta-analysis of host transcriptional responses to SARS-CoV-2 infection reveals their manifestation in human tumors. Sci Rep. 2021;11(1):2459.
8. Chen H, Qian Y, Chen X, Ruan Z, Ye Y, Chen H, Babiuk LA, Jung YS, Dai J. HDAC6 restricts influenza A virus by deacetylation of the RNA polymerase PA subunit. J Virol. 2019;93(4):10–1128.
9. Choi SJ, Lee HC, Kim JH, Park SY, Kim TH, Lee WK, Jang DJ, Yoon JE, Choi YI, Kim S, Ma J. HDAC 6 regulates cellular viral RNA sensing by deacetylation of RIG-I. EMBO J. 2016;35(4):429–42.
10. Cortese M, Lee JY, Cerikan B, Neufeldt CJ, Oorschot VM, Köhrer S, Hennies J, Schieber NL, Ronchi P, Mizzon G, Romero-Brey I. Integrative imaging reveals SARS-CoV-2-induced reshaping of subcellular morphologies. Cell Host Microbe. 2020;28(6):853–66.
11. Cubuk J, Alston JJ, Incicco JJ, Singh S, Stuchell-Brereton MD, Ward MD, Zimmerman MI, Vithani N, Griffith D, Wagoner JA, Bowman GR. The SARS-CoV-2 nucleocapsid protein is dynamic, disordered, and phase separates with RNA. Nat Commun. 2021;12(1):1936.
12. Dhama K, Khan S, Tiwari R, Sircar S, Bhat S, Malik YS, Singh KP, Chaicumpa W, Bonilla-Aldana DK, Rodriguez-Morales AJ. Coronavirus disease 2019–COVID-19. Clin Microbiol Rev. 2020;33(4):10–1128.
13. Ellis P, Somogyvári F, Virok DP, Noseda M, McLean GR. Decoding Covid-19 with the SARS-CoV-2 genome. Curr Genet Med Rep. 2021;9:1–12.
14. Gal J, Chen J, Na DY, Tichacek L, Barnett KR, Zhu H. The acetylation of lysine-376 of G3BP1 regulates RNA binding and stress granule dynamics. Mol Cell Biol. 2019;39(22):e00052-e119.
15. Gomes ID, Ariyaratne UV, Pflum MKH. HDAC6 substrate discovery using proteomics-based substrate trapping: HDAC6 deacetylates PRMT5 to influence methyltransferase activity. ACS Chem Biol. 2021;16(8):1435–44.
16. Gordon DE, Jang GM, Bouhaddou M, Xu J, Obernier K, White KM, O'Meara MJ, Rezelj VV, Guo JZ, Swaney DL, Tummino TA. A SARS-CoV-2 protein interaction map reveals targets for drug repurposing. Nature. 2020;583(7816):459–68.
17. Hatakeyama D, Masuda T, Miki R, Ohtsuki S, Kuzuhara T. In-vitro acetylation of SARS-CoV and SARS-CoV-2 nucleocapsid proteins by human PCAF and GCN5. Biochem Biophys Res Commun. 2021;557:273–9.
18. Hubbert C, Guardiola A, Shao R, Kawaguchi Y, Ito A, Nixon A, Yoshida M, Wang XF, Yao TP. HDAC6 is a microtubule-associated deacetylase. Nature. 2002;417(6887):455–8.
19. Husain M, Cheung CY. Histone deacetylase 6 inhibits influenza A virus release by downregulating the trafficking of viral components to the plasma membrane via its substrate, acetylated microtubules. J Virol. 2014;88(19):11229–39.
20. Katoh H, Okamoto T, Fukuhara T, Kambara H, Morita E, Mori Y, Kamitani W, Matsuura Y. Japanese encephalitis virus core protein inhibits stress granule formation through an interaction with Caprin-1 and facilitates viral propagation. J Virol. 2013;87(1):489–502.
21. Kawaguchi Y, Kovacs JJ, McLaurin A, Vance JM, Ito A, Yao TP. The deacetylase HDAC6 regulates aggresome formation and cell viability in response to misfolded protein stress. Cell. 2003;115(6):727–38.
22. Khaperskyy DA, Hatchette TF, McCormick C. Influenza A virus inhibits cytoplasmic stress granule formation. FASEB J. 2012;26(4):1629–39.
23. Kim D, Maharjan S, Kang M, Kim J, Park S, Kim M, Baek K, Kim S, Suh JG, Lee Y, Kwon HJ. Differential effect of SARS-CoV-2 infection on stress granule formation in Vero and Calu-3 cells. Front Microbiol. 2022;13:997539.
24. Kovacs JJ, Murphy PJ, Gaillard S, Zhao X, Wu JT, Nicchitta CV, Yoshida M, Toft DO, Pratt WB, Yao TP. HDAC6 regulates Hsp90 acetylation and chaperone-dependent activation of glucocorticoid receptor. Mol Cell. 2005;18:601–7. https://doi.org/10.1016/j.molcel.2005.04.021.
25. Kozlov MV, Kleymenova AA, Konduktorov KA, Malikova AZ, Kochetkov SN. Selective inhibitor of histone deacetylase 6 (tubastatin A) suppresses proliferation of hepatitis C virus replicon in culture of human hepatocytes. Biochemistry. 2014;79:637–42.
26. Kwon S, Zhang Y, Matthias P. The deacetylase HDAC6 is a novel critical component of stress granules involved in the stress response. Genes Dev. 2007;21:3381–94. https://doi.org/10.1101/gad.461107.
27. La Scola B, Le Bideau M, Andreani J, Hoang VT, Grimaldier C, Colson P, Gautret P, Raoult D. Viral RNA load as determined by cell culture as a management tool for discharge of SARS-CoV-2 patients from infectious disease wards. Eur J Clin Microbiol Infect Dis. 2020;39(6):1059–61.
28. Li Z, Xiao W, Yang Z, Guo J, Zhou J, Xiao S, Fang P, Fang L. Cleavage of HDAC6 to dampen its antiviral activity by nsp5 is a common strategy of swine enteric coronaviruses. J Virol. 2024;98(2):e01814-e1823.
29. Liu H, Bai Y, Zhang X, Gao T, Liu Y, Li E, Wang X, Cao Z, Zhu L, Dong Q, Hu Y. SARS-CoV-2 N protein antagonizes stress granule assembly and IFN production by interacting with G3BPs to facilitate viral replication. J Virol. 2022;96(12):e00412-e422.
30. Liu P, Xiao J, Wang Y, Song X, Huang L, Ren Z, Kitazato K, Wang Y. Post-translational modification and beyond: interplay between histone deacetylase 6 and heat-shock protein 90. Mol Med. 2021;27(1):1–12.
31. Liu Y, Qin C, Rao Y, Ngo C, Feng JJ, Zhao J, Zhang S, Wang TY, Carriere J, Savas AC, Zarinfar M. SARS-CoV-2 NSP5 demonstrates two distinct mechanisms targeting RIG-I and MAVS to evade the innate immune response. MBio. 2021;12(5):10–1128.
32. Lu CY, Chang YC, Hua CH, Chuang C, Huang SH, Kung SH, Hour MJ, Lin CW. Tubacin, an HDAC6 selective inhibitor, reduces the replication of the Japanese encephalitis virus via the decrease of viral RNA synthesis. Int J Mol Sci. 2017;18(5):954.
33. Marrero-Hernández S, Márquez-Arce D, Cabrera-Rodríguez R, Estévez-Herrera J, Pérez-Yanes S, Barroso-González J, Madrid R, Machado JD, Blanco J, Valenzuela-Fernández A. HIV-1 nef targets HDAC6 to assure viral production and virus infection. Front Microbiol. 2019;10:2437.
34. Miller CL. Stress granules and virus replication. Future Virol. 2011;6(11):1329–38.
35. Moffat J, Grueneberg DA, Yang X, Kim SY, Kloepfer AM, Hinkle G, Piqani B, Eisenhaure TM, Luo B, Grenier JK, Carpenter AE. A lentiviral RNAi library for human and mouse genes applied to an arrayed viral high-content screen. Cell. 2006;124(6):1283–98.
36. Nabeel-Shah S, Lee H, Ahmed N, Burke GL, Farhangmehr S, Ashraf K, Pu S, Braunschweig U, Zhong G, Wei H, Tang H. SARS-CoV-2 nucleocapsid

Mukherjee *et al. Virology Journal*   (2024) 21:186

Page 16 of 16

protein binds host mRNAs and attenuates stress granules to impair host stress response. iScience. 2022;25(1):103562.

37. Nelson EV, Schmidt KM, Deflubé LR, Doğanay S, Banadyga L, Olejnik J, Hume AJ, Ryabchikova E, Ebihara H, Kedersha N, Ha T. Ebola virus does not induce stress granule formation during infection and sequesters stress granule proteins within viral inclusions. J Virol. 2016;90(16):7268–84.

38. Nusinzon I, Horvath CM. Positive and negative regulation of the innate antiviral response and beta interferon gene expression by deacetylation. Mol Cell Biol. 2006;26(8):3106–13.

39. Onomoto K, Yoneyama M, Fung G, Kato H, Fujita T. Antiviral innate immunity and stress granule responses. Trends Immunol. 2014;35(9):420–8.

40. Partridge LJ, Urwin L, Nicklin MJ, James DC, Green LR, Monk PN. ACE2-independent interaction of SARS-CoV-2 spike protein with human epithelial cells is inhibited by unfractionated heparin. Cells. 2021;10(6):1419.

41. Patra T, Meyer K, Geerling L, Isbell TS, Hoft DF, Brien J, Pinto AK, Ray RB, Ray R. SARS-CoV-2 spike protein promotes IL-6 trans-signaling by activation of angiotensin II receptor signaling in epithelial cells. PLoS Pathog. 2020;16(12):e1009128.

42. Saito M, Hess D, Eglinger J, Fritsch AW, Kreysing M, Weinert BT, Choudhary C, Matthias P. Acetylation of intrinsically disordered regions regulates phase separation. Nat Chem Biol. 2019;15(1):51–61.

43. Schaefer JB, Morgan DO. Protein-linked ubiquitin chain structure restricts activity of deubiquitinating enzymes. J Biol Chem. 2011;286(52):45186–96.

44. Shen S, Kozikowski AP. A patent review of histone deacetylase 6 inhibitors in neurodegenerative diseases (2014–2019). Expert Opin Ther Pat. 2020;30(2):121–36.

45. Shih HW, Tsao CH, Chang YH, Yang CW, Feng SW, Chiu KC. A selective histone deacetylase 6 inhibitor showed antiviral activity against dengue and Zika viruses. J Med Sci. 2023;43(5):219–26.

46. Shin HJ, DeCotiis J, Giron M, Palmeri D, Lukac DM. Histone deacetylase classes I and II regulate Kaposi's sarcoma-associated herpesvirus reactivation. J Virol. 2014;88(2):1281–92.

47. Tsai WC, Lloyd RE. Cytoplasmic RNA granules and viral infection. Annu Rev Virol. 2014;1:147–70.

48. Twu WI, Lee JY, Kim H, Prasad V, Cerikan B, Haselmann U, Tabata K, Bartenschlager R. Contribution of autophagy machinery factors to HCV and SARS-CoV-2 replication organelle formation. Cell Rep. 2021;37(8):110049.

49. Valera MS, de Armas-Rillo L, Barroso-González J, Ziglio S, Batisse J, Dubois N, Marrero-Hernandez S, Borel S, García-Expósito L, Biard-Piechaczyk M, Paillart JC. The HDAC6/APOBEC3G complex regulates HIV-1 infectiveness by inducing Vif autophagic degradation. Retrovirology. 2015;12:1–26.

50. Visser LJ, Langereis MA, Rabouw HH, Wahedi M, Muntjewerff EM, de Groot RJ, van Kuppeveld FJ. Essential role of enterovirus 2A protease in counteracting stress granule formation and the induction of type I interferon. J Virol. 2019;93(10):e00222-e319.

51. Visser LJ, Medina GN, Rabouw HH, de Groot RJ, Langereis MA, de Los Santos T, van Kuppeveld FJ. Foot-and-mouth disease virus leader protease cleaves G3BP1 and G3BP2 and inhibits stress granule formation. J Virol. 2019;93(2):10–1128.

52. Wang L, Moreira EA, Kempf G, Miyake Y, Esteves BIO, Fahmi A, Schaefer JV, Dreier B, Yamauchi Y, Alves MP, Plückthun A. Disrupting the HDAC6-ubiquitin interaction impairs infection by influenza and Zika virus and cellular stress pathways. Cell Rep. 2022;39(4):110736.

53. WHO COVID-19 Dashboard. Geneva: World Health Organization, 2020. Available online: https://covid19.who.int/.

54. Wu J, Shi Y, Pan X, Wu S, Hou R, Zhang Y, Zhong T, Tang H, Du W, Wang L, Wo J. SARS-CoV-2 ORF9b inhibits RIG-I-MAVS antiviral signaling by interrupting K63-linked ubiquitination of NEMO. Cell Rep. 2021;34(7):108761.

55. Yoneyama M, Jogi M, Onomoto K. Regulation of antiviral innate immune signaling by stress-induced RNA granules. J Biochem. 2016;159(3):279–86.

56. Yoshida N, Omoto Y, Inoue A, Eguchi H, Kobayashi Y, Kurosumi M, Saji S, Suemasu K, Okazaki T, Nakachi K, Fujita T. Prediction of prognosis of estrogen receptor-positive breast cancer with combination of selected estrogen-regulated genes. Cancer Sci. 2004;95(6):496–502.

57. Yoshimoto FK. The proteins of severe acute respiratory syndrome coronavirus-2 (SARS CoV-2 or n-COV19), the cause of COVID-19. Protein J. 2020;39(3):198–216.

58. Zhang X, Yuan Z, Zhang Y, Yong S, Salas-Burgos A, Koomen J, Olashaw N, Parsons JT, Yang XJ, Dent Yao SRTP, Lane WS, Seto E. HDAC6 modulates cell motility by altering the acetylation level of cortactin. Mol Cell. 2007;27:197–213. https://doi.org/10.1016/j.molcel.2007.05.033.

59. Zhang Y, Li N, Caron C, Matthias G, Hess D, Khochbin S, Matthias P. HDAC-6 interacts with and deacetylates tubulin and microtubules in vivo. EMBO J. 2003;22(5):1168–79.

60. Zheng K, Jiang Y, He Z, Kitazato K, Wang Y. Cellular defence or viral assist: the dilemma of HDAC6. J Gen Virol. 2017;98(3):322–37.

61. Zheng Y, Zhu G, Tang Y, Yan J, Han S, Yin J, Peng B, He X, Liu W. HDAC6, a novel cargo for autophagic clearance of stress granules, mediates the repression of the Type I interferon response during coxsackievirus A16 infection. Front Microbiol. 2020;11:78.

62. Zheng ZQ, Wang SY, Xu ZS, Fu YZ, Wang YY. SARS-CoV-2 nucleocapsid protein impairs stress granule formation to promote viral replication. Cell Discov. 2021;7(1):38.

63. Zheng Y, Deng J, Han L, Zhuang MW, Xu Y, Zhang J, Nan ML, Xiao Y, Zhan P, Liu X, Gao C. SARS-CoV-2 NSP5 and N protein counteract the RIG-I signaling pathway by suppressing the formation of stress granules. Signal Transduct Targeted Ther. 2022;7(1):22.

64. Zhu J, Coyne CB, Sarkar SN. PKC alpha regulates Sendai virus-mediated interferon induction through HDAC6 and β-catenin. EMBO J. 2011;30(23):4838–49.

65. Zong S, Wu Y, Li W, You Q, Peng Q, Wang C, Wan P, Bai T, Ma Y, Sun B, Qiao J. SARS-CoV-2 NSP8 induces mitophagy by damaging mitochondria. Virol Sin. 2023;38:520–30.

Publisher's Note